frontiers in Energy Research

BRIEF RESEARCH REPORT
published: 27 August 2020
doi: 10.3389/fenrg.2020.00199

Polypyrrole Wrapped V_2O_5 Nanowires Composite for Advanced Aqueous Zinc-Ion Batteries

Xinghua Qin[1], Xinyu Wang[1]*, Juncai Sun[1], Qiongqiong Lu[2]*, Ahmad Omar[2] and Daria Mikhailova[2]

[1] Institute of Materials and Technology, Dalian Maritime University, Dalian, China, [2] Leibniz Institute for Solid State and Materials Research (IFW) Dresden e.V., Dresden, Germany

OPEN ACCESS

Edited by:
Yaolin Xu,
Helmholtz-Zentrum Berlin für Materialien und Energie, Helmholtz-Gemeinschaft Deutscher Forschungszentren (HZ), Germany

Reviewed by:
Soorathep Kheawhom,
Chulalongkorn University, Thailand
Lian Yi Shao,
Guangdong University of Technology, China
Ning Zhang,
Hebei University, China

***Correspondence:**
Xinyu Wang
wangxinyu@dlmu.edu.cn
Qiongqiong Lu
q.lu@ifw-dresden.de

Specialty section:
This article was submitted to Electrochemical Energy Conversion and Storage, a section of the journal Frontiers in Energy Research

Received: 01 July 2020
Accepted: 29 July 2020
Published: 27 August 2020

Citation:
Qin X, Wang X, Sun J, Lu Q, Omar A and Mikhailova D (2020) Polypyrrole Wrapped V_2O_5 Nanowires Composite for Advanced Aqueous Zinc-Ion Batteries. Front. Energy Res. 8:199. doi: 10.3389/fenrg.2020.00199

Aqueous zinc-ion batteries (ZIBs) have obtained increasing attention owing to the high safety, material abundance, and environmental benignity. However, the development of cathode materials with high capacity and stable cyclability is still a challenge. Herein, the polypyrrole (PPy)-wrapped V_2O_5 nanowire (V_2O_5/PPy) composite was synthesized by a surface-initiated polymerization strategy, ascribing to the redox reaction between V_2O_5 and pyrrole. The introduction of PPy on the surface of V_2O_5 nanowires not only enhanced the electronic conductivity of the active materials but also reduced the V_2O_5 dissolution. As a result, the V_2O_5/PPy composite cathode exhibits a high specific capacity of 466 mAh g^{-1} at 0.1 A g^{-1} and a superior cycling stability with 95% capacity retention after 1000 cycles at a high current density of 5 A g^{-1}. The superior electrochemical performance is ascribed to the large ratio of capacitive contribution (92% at 1 mV s^{-1}) and a fast Zn^{2+} diffusion rate. This work presents a simple method for fabricating V_2O_5/PPy composite toward advanced ZIBs.

Keywords: V_2O_5 nanowires, surface-initiated polymerization, polypyrrole, cathode material, aqueous zinc-ion battery

INTRODUCTION

The ever-increasing energy consumption, and limited fossil fuels, necessitates effective utilization of renewable energy resources (Xu F. et al., 2020). For that purpose, large-scale efficient energy storage systems are desired (Shao et al., 2021). Although lithium-ion battery has found widespread applicability, it suffers from safety issues caused by flammable organic electrolytes as well as the availability of Li source (Dong et al., 2020; Lu et al., 2020). Aqueous zinc-ion batteries (ZIBs) are regarded as a suitable alternative for scalable energy storage systems, due to the usage of zinc metal anode which, apart from high abundance and environmental friendliness, has a large theoretical capacity (820 mAh g^{-1}) and a low redox potential [−0.76 V vs. SHE (Wang F. et al., 2018; Wang et al., 2020b; Zhang et al., 2019a). Furthermore, the possibility of an aqueous electrolyte endows an intrinsic non-flammability and high ionic conductivity (Wang et al., 2020a). However, corresponding ZIB cathode materials with high capacity and stable cyclability need to be further explored (Zhang et al., 2019b).

Manganese oxides (Khamsanga et al., 2019; Wang J. et al., 2019), Prussian blue analogs (Liu et al., 2020; Zampardi and La Mantia, 2020), vanadium-based compounds (Yang et al., 2020), and some organic materials (Wang et al., 2020c) have been investigated as cathode materials for aqueous

ZIBs. Among those, vanadium-based materials, particularly vanadium oxides, are very attractive because of the advantage of high theoretical capacities due to multiple oxidation states of vanadium. Unfortunately, the electrochemical performance of vanadium oxides in ZIBs is hindered by their poor electronic conductivity and noticeable solubility in the electrolyte (Zhang et al., 2020). To address these issues, various strategies have been applied, such as using pre-insertion materials ($V_2O_5 \cdot H_2O$) (Wang X. et al., 2019), integration with carbon materials (Yan et al., 2018), as well as electrolyte modifications (Wan et al., 2018). Another viable approach is to incorporate conducting polymers along with V_2O_5 (Du et al., 2020). Polypyrrole (PPy) is a widely used conductive polymer, and V_2O_5/PPy composites have been shown to exhibit enhanced performance in supercapacitors and LIBs (Wang J.G. et al., 2018). Therefore, with regard to aqueous ZIBs, an effective PPy coating can aid in enhancing the electronic conductivity of V_2O_5 as well as help to reduce the solubility in the electrolyte.

Herein, V_2O_5 nanowires were synthesized by a facile hydrothermal method, and a surface-initiated polymerization method was utilized to fabricate a PPy-wrapped V_2O_5 nanowire composite. V_2O_5 served as the initiator to induce the polymerization reaction of pyrrole monomer at room temperature due to the strong oxidizing property of V^{5+}. Benefiting from the improved electronic conductivity and restricted V_2O_5 dissolution due to the PPy layer, V_2O_5/PPy cathode delivered a higher specific capacity and rate performance in comparison to the pristine V_2O_5 nanowire cathode. Therefore, the V_2O_5/PPy composite is a promising high-performance cathode material for aqueous ZIBs toward large-scale energy storage applications.

EXPERIMENTAL SECTION

V_2O_5 nanowires were synthesized by a facile hydrothermal method according to previously reported literature (Wang J.G. et al., 2018). 200 mg of obtained V_2O_5 nanowires was dispersed into deionized water. Then, pyrrole (0.1 ml) dissolved in DMF (4 ml) was slowly added to the above V_2O_5 nanowire suspended solution and stirred for 24 h. The obtained V_2O_5/PPy was washed carefully and dried in a vacuum oven.

More detailed synthesis and characterization processes are available in electronic **Supplementary Information**.

RESULTS AND DISCUSSION

V_2O_5 nanowires were synthesized by the hydrothermal method. The as-obtained V_2O_5 nanowires show a diameter of approximately 15 nm with a cable-like nanostructure (**Supplementary Figure S1A**). The V_2O_5/PPy composites were prepared using a surface-initiated polymerization strategy, as shown in **Figure 1A**. Owing to the strong oxidizing property of V_2O_5, the pyrrole monomer can be polymerized with V_2O_5 initiation, resulting in the surface coating of V_2O_5 with PPy. The morphology of V_2O_5 nanowires was well-maintained after PPy coating, indicating that the wrapping procedure has no significant influence on the V_2O_5 morphology (**Figure 1B**). The TEM image also confirms the nanowire morphology of the V_2O_5/PPy composite (**Figure 1D**). EDS elemental mappings show the homogeneous distribution of C, O, V, and N throughout the entire V_2O_5/PPy composite, indicating the presence of PPy (**Figure 1C** and **Supplementary Figure S1B**).

The XRD data of the V_2O_5 nanowires mainly fit with the layered orthorhombic structure (JCPDS no. 40-1296), and typical (001) and (003) reflection peaks are present (**Figure 1E**). A little amount of V_4O_7 was also indexed and may be assigned to the reduction of P123. The interlayer distance is estimated to be 0.96 nm by Bragg's law from the (001) peak. This large distance is beneficial for Zn^{2+} insertion/extraction during the electrochemical process. After the PPy coating, no significant change is observed in the XRD data, indicating that the layered structure was well maintained after the polymerization process. In order to confirm the PPy coating and identify the valence state of vanadium in the V_2O_5/PPy composite, XPS was carried out. **Figure 1F** shows the survey spectrum with the clear presence of N 1s and C 1s, confirming the polymeric coating (see also **Supplementary Figure S2**). **Figure 1G** shows the V 2p spectrum, with strong V 2p3/2 and V 2p1/2 peaks of V^{5+} located at 517.6 eV and 525 eV, along with shoulder peaks at 516 eV and 523.8 eV, corresponding to V^{4+} (Liu et al., 2019). The presence of a small amount of V^{4+} (9.3 at.%) corresponds to the oxygen vacancies generated in the V_2O_5 surface due to the redox reaction between V_2O_5 and pyrrole. Previous studies on V_2O_5 demonstrated that such vacancies enhance the electrochemical performance (Liao et al., 2020).

The electrochemical performance of pristine V_2O_5 and V_2O_5/PPy composites is evaluated in aqueous ZIBs. **Figure 2A** presents the rate capability of the pristine V_2O_5 cathode and V_2O_5/PPy composite cathode. The V_2O_5/PPy composite cathode delivers a high initial capacity of 466 mAh g^{-1} at 0.1 A g^{-1}, as compared to the V_2O_5 nanowire electrodes (425 mAh g^{-1}). Even at a very high current density of 5.0 A g^{-1}, the V_2O_5/PPy composite cathode still possesses a higher discharge capacity of 174 mAh g^{-1} than that observed for the V_2O_5 nanowire cathode (142 mAh g^{-1}). The results point to the better rate performance of V_2O_5/PPy composite in comparison to non-modified V_2O_5 nanowire electrodes. The voltage-capacity plots for the V_2O_5/PPy composite at different current rates demonstrate that the redox plateaus are well maintained even at a high current density of 5.0 A g^{-1} (**Figure 2B**). In comparing to voltage-capacity plots for pristine V_2O_5, the overpotentials are slightly lower suggesting improved kinetics due to the higher electrical conductivity of the composite (**Supplementary Figure S3**).

Based on the voltage profiles, the energy/power densities of the batteries were calculated and are shown in the Ragone plot (**Figure 2C**). Impressively, the batteries base on the V_2O_5/PPy composite cathode display a high energy density of 235 Wh kg^{-1} at a power density of 56 W kg^{-1} and exhibit a relatively high energy density of 100 Wh kg^{-1} even at a high power density of 2335 W kg^{-1}. Moreover, the V_2O_5/PPy composite cathodes are highly competitive among the aqueous ZIBs based on the different cathodes: V_2O_5 (Hu et al., 2017),

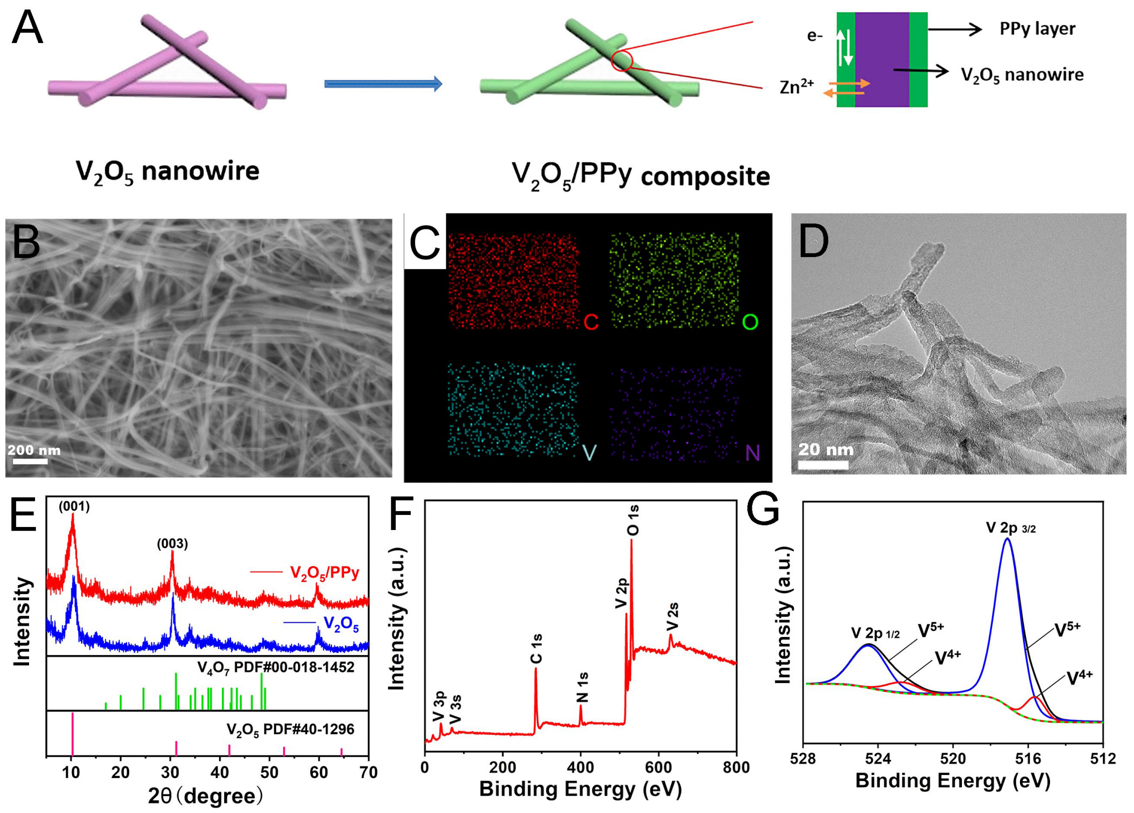

FIGURE 1 | (A) Schematic illustrating the preparation of V_2O_5/PPy composite. Characterizations of the V_2O_5/PPy composite. **(B)** SEM image and **(C)** Corresponding elemental mappings, **(D)** TEM image, **(E)** XRD patterns, **(F)** XPS survey spectrum, and **(G)** V 2p spectrum with fitting showing mixed valence of V after PPy coating.

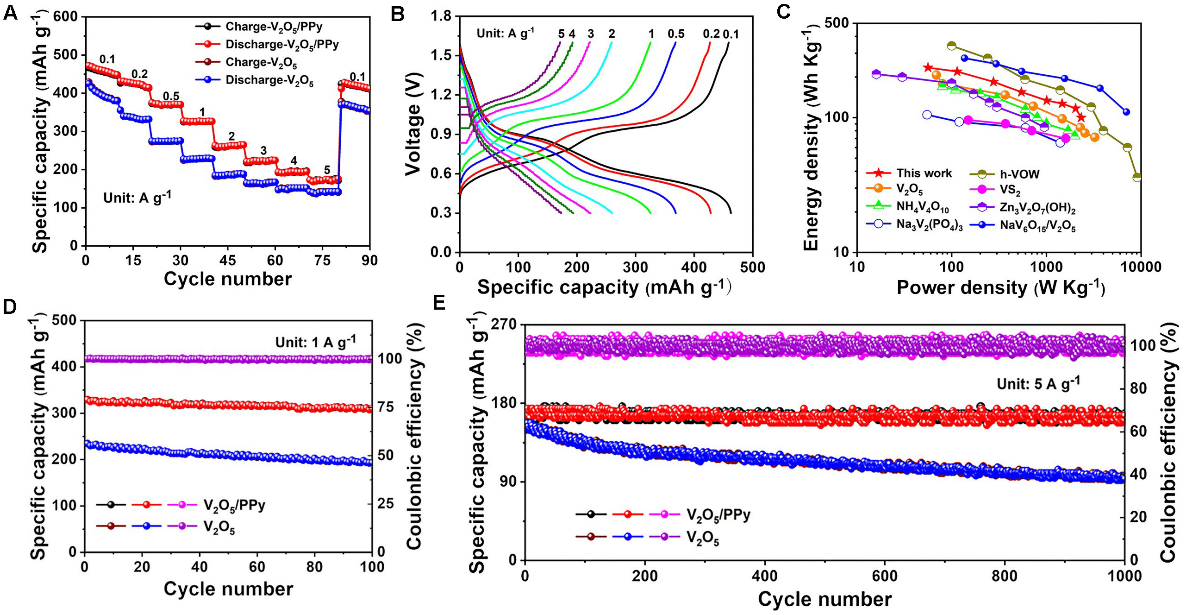

FIGURE 2 | Electrochemical performance of V_2O_5/PPy composites cathode in aqueous ZIBs. **(A)** Rate performance in comparison to pristine V_2O_5. **(B)** Voltage profile plots at different current rates. **(C)** Ragone plot. **(D)** Cycling performance at 1A g^{-1} and **(E)** Long-term cycling performance at 5A g^{-1}, in comparison to pristine V_2O_5.

TABLE 1 | Comparison of the initial capacity and cycling stability of V_2O_5/PPy composite with recent literature data on vanadium oxide-based cathodes in aqueous ZIBs.

Electrodes	Rate ($mA\ g^{-1}$)	Initial capacity ($mAh\ g^{-1}$)	Capacity Retention	References
V_2O_5/PPy	1000	329	94% (100 cycles)	This work
	5000	174	95% (1000 cycles)	
$K_{0.25}V_2O_5$	1000	205	83% (50 cycles)	Li S. et al., 2019
$Na_{1.25}V_3O_8$	1000	280	75% (50 cycles)	Xie et al., 2020
α-$Zn_2V_2O_7$	4000	163	85% (1000 cycles)	Sambandam et al., 2018
$V_2O_5{\cdot}nH_2O$	6000	281.7	71% (900 cycles)	Yan et al., 2018
$H_2V_3O_8$	5000	173.6	94.3% (1000 cycles)	He et al., 2017a
$Li_xV_2O_5{\cdot}nH_2O$	5000	252	92.1% (500 cycles)	Yang Y. et al., 2018
$(NH_4)_2V_6O_{16}$	1000	361.6	76.1% (100 cycles)	Xu L. et al., 2020

$NH_4V_4O_{10}$ (Yang G. et al., 2018), $Na_3V_2(PO_4)_3$ (Li et al., 2016), heterogeneous vanadium oxide nanowire with $V_2O_5{\cdot}nH_2O$ shell and $V_3O_7{\cdot}H_2O$ core (h-VOW) (Li X. et al., 2019), VS_2 (He et al., 2017b), $Zn_3V_2O_7(OH)_2$ (Chao et al., 2018), and NaV_6O_{15}/V_2O_5 (Lanlan et al., 2020). In addition, as shown in **Figure 2D**, the V_2O_5/PPy composite cathode exhibits a high initial capacity of 329 mAh g^{-1} at 1 A g^{-1} and a capacity retention of 94% after 100 cycles, which is much higher than that of pristine V_2O_5 cathodes (234 mAh g^{-1}, 82%). Furthermore, long-term cycling performance of the cathodes was evaluated, because it is a key feature for practical applications. Even after 1000 cycles, the batteries based on the V_2O_5/PPy composite cathode show a reversible capacity of 174 mAh g^{-1} with a capacity retention of 95%. In contract, pristine V_2O_5 cathodes exhibit a poor cycling stability, with a specific capacity of only 93 mAh g^{-1} after 1000 cycles corresponding to a capacity retention of 62% (**Figure 2E**). The strong capacity fading observed for pristine V_2O_5 cathode is most probably be a result of V_2O_5 dissolution during cycling, which is minimized with the PPy coating for the V_2O_5/PPy composite. Moreover, such a high cycling stability for the V_2O_5/PPy composite is better compared to the recently reported literature on aqueous ZIBs with vanadium oxide-based cathodes (**Table 1**). The high rate performance and stable long cycle life of the V_2O_5/PPy composite cathode are ascribed to the introduction of a conductive polymer PPy layer, which not only increases the electronic conductivity but also reduces the dissolution of V_2O_5 in the electrolyte.

The electrochemical kinetics of the V_2O_5/PPy composite cathode was further investigated to understand the impressive performance. Cyclic voltammetry (CV) was performed at various scan rates from 0.1 to 1.0 mV s^{-1} (**Figure 3A**). The CV curves show similar redox peaks in the voltage window of 0.3–1.6 V. The characteristic peaks appeared at 0.5/0.7 V as well as 0.8/1.0 V,

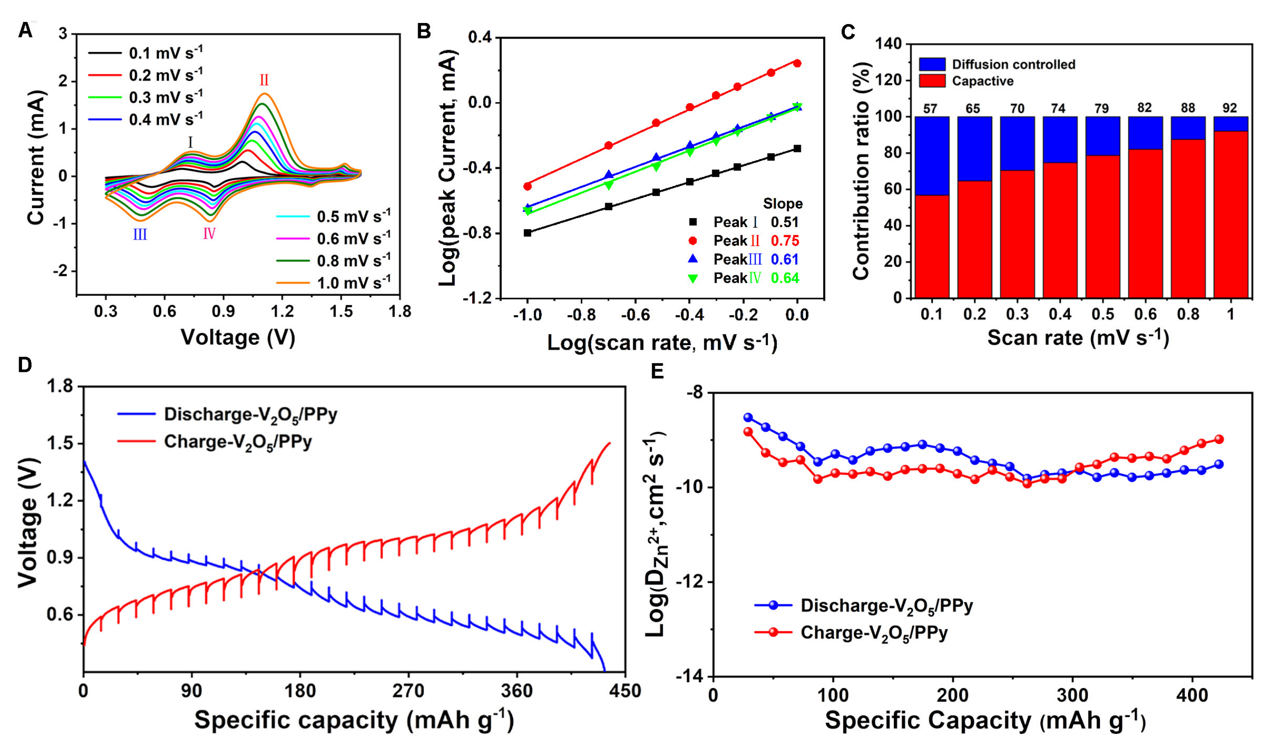

FIGURE 3 | The electrochemical kinetics of the V_2O_5/PPy composite cathode. **(A)** CV curves at different scan rates. **(B)** Log(peak current) vs. log(scan rate) plots for different peaks marked in **(A)**. **(C)** Capacity contribution ratios at different scan rates. **(D)** GITT curves. **(E)** Evaluated diffusion coefficients of Zn^{2+}.

reflecting the redox processes in V_2O_5 that is consistent with reported literature (Yang Y. et al., 2018; Zhang et al., 2018). The capacity is regarded to be originated from two contributed parts: a surface-controlled capacitive part and a diffusion-induced part, as described in the literature (Ming et al., 2018):

$$i = av^b \tag{1}$$

In this equation, v is the scan rate, and a and b refer to adjustable parameters. The b values range from 0.5 to 1.0. Corresponding to $b = 0.5$, the observed capacity is fully diffusion-induced. When the capacity is completely determined by a surface-controlled capacitive part, the b value is close to 1.0. The peak currents at different scan rates are plotted and fitted with a linear function (**Figure 3B**). The b values are 0.51, 0.75, 0.61, and 0.64, which implies that the capacity of the V_2O_5/PPy composite cathode is simultaneously influenced by both the capacitive and diffusion processes. Furthermore, the capacity is divided as a capacitive-controlled part (k_1v) and diffusion-induced part ($k_2v^{1/2}$) as described by the following equations:

$$i = k_1v + k_2v^{1/2} \tag{2}$$

or

$$i/v^{1/2} = k_1v^{1/2} + k_2 \tag{3}$$

The ratios of surface-controlled capacitive and diffusion-induced parts with various scan rates are displayed in **Figure 3C**. The surface-controlled capacitive contribution ratio increases from 57% (0.1 mV s^{-1}) to 92% (1.0 mV s^{-1}), indicating that the batteries possess fast charge-transfer kinetics. The kinetics of the V_2O_5/PPy composite cathode is further evaluated by galvanostatic intermittent titration technique (GITT). The profiles in GITT curves of V_2O_5/PPy electrode are well in coincidence with the galvanostatic charge–discharge profiles (**Figure 3D**). The zinc-ion diffusion coefficient during discharging–charging procedures for V_2O_5/PPy is 3.03×10^{-9}–1.46×10^{-10} cm^2 S^{-1} (**Figure 3E**), which is comparable to that of the reported aqueous ZIBs based on the V_2O_5@CNT composite and porous V_2O_5 nanofiber cathodes (Chen et al., 2019, 2020).

CONCLUSION

In this work, a surface-initiated polymerization strategy was utilized to synthesize PPy-wrapped V_2O_5 nanowires. Owing to the strong oxidizing property of V^{5+}, the polymerization of the pyrrole monomer could be initiated at room temperature. Due to the introduction of the conductive PPy layer, the V_2O_5/PPy cathode displayed a superior specific capacity and excellent cycling stability. The outstanding electrochemical properties are explained by the large ratio of a capacitive-controlled process (92% at 1 mV s^{-1}) and a fast zinc ion diffusion coefficient. Considering the excellent electrochemical performance, coupled with the safe and simple operation process of aqueous ZIBs, the V_2O_5/PPy composite cathode holds great promise for practical grid-level storage applications.

DATA AVAILABILITY STATEMENT

The raw data supporting the conclusions of this article will be made available by the authors, without undue reservation.

AUTHOR CONTRIBUTIONS

All authors listed have made a substantial, direct and intellectual contribution to the work, and approved it for publication.

FUNDING

This work was supported by the National Natural Science Foundation of China (21905037) and the Fundamental Research Funds for the Central Universities (3132019328 and 3132020151).

ACKNOWLEDGMENTS

QL acknowledges the financial support from the China Scholarship Council (CSC).

SUPPLEMENTARY MATERIAL

The Supplementary Material for this article can be found online at: https://www.frontiersin.org/articles/10.3389/fenrg.2020.00199/full#supplementary-material

REFERENCES

Chao, D., Zhu, C., Song, M., Liang, P., Zhang, X., Tiep, N. H., et al. (2018). A high-rate and stable quasi-solid-state zinc-ion battery with novel 2D layered zinc orthovanadate array. *Adv. Mater.* 30:1803181. doi: 10.1002/adma.201803181

Chen, H., Qin, H., Chen, L., Wu, J., and Yang, Z. (2020). V2O5@CNTs as cathode of aqueous zinc ion battery with high rate and high stability. *J. Alloys Compd.* 842, 1–7. doi: 10.1016/j.jallcom.2020.155912

Chen, X., Wang, L., Li, H., Cheng, F., and Chen, J. (2019). Porous V2O5 nanofibers as cathode materials for rechargeable aqueous zinc-ion batteries. *J. Energy Chem.* 38, 20–25. doi: 10.1016/j.jechem.2018.12.023

Dong, Y., Di, S., Zhang, F., Bian, X., Wang, Y., Xu, J., et al. (2020). Nonaqueous electrolyte with dual-cations for high-voltage and long-life zinc batteries. *J. Mater. Chem. A* 8, 3252–3261. doi: 10.1039/c9ta13068c

Du, Y., Wang, X., Man, J., and Sun, J. (2020). A novel organic-inorganic hybrid V2O5@polyaniline as high-performance cathode for aqueous zinc-ion batteries. *Mater. Lett.* 272:127813. doi: 10.1016/j.matlet.2020.127813

He, P., Quan, Y., Xu, X., Yan, M., Yang, W., An, Q., et al. (2017a). High-performance aqueous zinc-Ion battery based on layered H2V3O8 nanowire cathode. *Small* 13:1702551. doi: 10.1002/smll.201702551

He, P., Yan, M., Zhang, G., Sun, R., Chen, L., An, Q., et al. (2017b). Layered VS2 nanosheet-based aqueous Zn ion battery cathode. *Adv. Energy Mater.* 7:1601920. doi: 10.1002/aenm.201601920

Hu, P., Yan, M., Zhu, T., Wang, X., Wei, X., Li, J., et al. (2017). Zn/V2O5 aqueous hybrid-ion battery with high voltage platform and long cycle life. *ACS Appl. Mater. Interfaces* 9, 42717–42722. doi: 10.1021/acsami.7b13110

Khamsanga, S., Pornprasertsuk, R., Yonezawa, T., Mohamad, A. A., and Kheawhom, S. (2019). delta-MnO2 nanoflower/graphite cathode for rechargeable aqueous zinc ion batteries. *Sci. Rep.* 9:8441. doi: 10.1038/s41598-019-44915-8

Lanlan, F., Zhenhuan, L., Weimin, K., and Bowen, C. (2020). Highly stable aqueous rechargeable Zn-ion battery: the synergistic effect between NaV6O15 and V2O5 in skin-core heterostructured nanowires cathode. *J. Energy Chem.* 55, 25–33. doi: 10.1016/j.jechem.2020.06.075

Li, G., Yang, Z., Jiang, Y., Jin, C., Huang, W., Ding, X., et al. (2016). Towards polyvalent ion batteries: a zinc-ion battery based on NASICON structured Na3V2(PO4)3. *Nano Energy* 25, 211–217. doi: 10.1016/j.nanoen.2016.04.051

Li, S., Chen, M., Fang, G., Shan, L., Cao, X., Huang, J., et al. (2019). Synthesis of polycrystalline K0.25V2O5 nanoparticles as cathode for aqueous zinc-ion battery. *J. Alloys Compd.* 801, 82–89. doi: 10.1016/j.jallcom.2019.06.084

Li, X., Ma, L., Zhao, Y., Yang, Q., Wang, D., Huang, Z., et al. (2019). Hydrated hybrid vanadium oxide nanowires as the superior cathode for aqueous Zn battery. *Mater. Today Energy* 14, 1–7. doi: 10.1016/j.mtener.2019.100361

Liao, M., Wang, J., Ye, L., Sun, H., Wen, Y., Wang, C., et al. (2020). A deep-cycle aqueous zinc-ion battery containing an oxygen-deficient vanadium oxide cathode. *Angew. Chem. Int. Ed.* 59, 2273–2278. doi: 10.1002/anie.201912203

Liu, C., Sun, Y., Nie, J., Dong, D., Xie, J., and Zhao, X. (2020). Stable cycling of a prussian blue-based Na/Zn hybrid battery in aqueous electrolyte with a wide electrochemical window. *New J. Chem.* 44, 4639–4646. doi: 10.1039/c9nj06024c

Liu, F., Chen, Z., Fang, G., Wang, Z., Cai, Y., Tang, B., et al. (2019). V2O5 nanospheres with mixed vanadium valences as high electrochemically active aqueous zinc-ion battery cathode. *Nano Micro Lett.* 11:25. doi: 10.1007/s40820-019-0256-2

Lu, Q., Wang, X., Omar, A., and Mikhailova, D. (2020). 3D Ni/Na metal anode for improved sodium metal batteries. *Mater. Lett.* 275, 128206–128210. doi: 10.1016/j.matlet.2020.128206

Ming, F., Liang, H., Lei, Y., Kandambeth, S., Eddaoudi, M., and Alshareef, H. N. (2018). Layered MgxV2O5·nH2O as cathode material for high-performance aqueous zinc ion batteries. *ACS Energy Lett.* 3, 2602–2609. doi: 10.1021/acsenergylett.8b01423

Sambandam, B., Soundharrajan, V., Kim, S., Alfaruqi, M. H., Jo, J., Kim, S., et al. (2018). Aqueous rechargeable Zn-ion batteries: an imperishable and high-energy Zn2V2O7 nanowire cathode through intercalation regulation. *J. Mater. Chem. A* 6, 3850–3856. doi: 10.1039/C7TA11237H

Shao, L., Wang, S., Wu, F., Shi, X., Sun, Z., and Tang, Y. (2021). Pampas grass-inspired FeOOH nanobelts as high performance anodes for sodium ion batteries. *J. Energy Chem.* 54, 138–142. doi: 10.1016/j.jechem.2020.05.051

Wan, F., Zhang, L., Dai, X., Wang, X., Niu, Z., and Chen, J. (2018). Aqueous rechargeable zinc/sodium vanadate batteries with enhanced performance from simultaneous insertion of dual carriers. *Nat. Commun.* 9:1656. doi: 10.1038/s41467-018-04060-8

Wang, F., Borodin, O., Gao, T., Fan, X., Sun, W., Han, F., et al. (2018). Highly reversible zinc metal anode for aqueous batteries. *Nat. Mater.* 17, 543–549. doi: 10.1038/s41563-018-0063-z

Wang, J.-G., Liu, H., Liu, H., Hua, W., and Shao, M. (2018). Interfacial constructing flexible V2O5@polypyrrole core–shell nanowire membrane with superior supercapacitive performance. *ACS Appl. Mater. Interfaces* 10, 18816–18823. doi: 10.1021/acsami.8b05660

Wang, J., Wang, J.-G., Liu, H., Wei, C., and Kang, F. (2019). Zinc ion stabilized MnO2 nanospheres for high capacity and long lifespan aqueous zinc-ion batteries. *J. Mater. Chem. A* 7, 13727–13735. doi: 10.1039/c9ta03541a

Wang, X., Ma, L., and Sun, J. (2019). Vanadium pentoxide nanosheets in-situ spaced with acetylene black as cathodes for high-performance zinc-ion batteries. *ACS Appl. Mater. Interfaces* 11, 41297–41303. doi: 10.1021/acsami.9b13103

Wang, X., Li, Y., Wang, S., Zhou, F., Das, P., Sun, C., et al. (2020a). 2D Amorphous V2O5/graphene heterostructures for high-safety aqueous Zn-ion batteries with unprecedented capacity and ultrahigh rate capability. *Adv. Energy Mater.* 10:2000081. doi: 10.1002/aenm.202000081

Wang, X., Qin, X., Lu, Q., Han, M., Omar, A., and Mikhailova, D. (2020b). Mixed phase sodium manganese oxide as cathode for enhanced aqueous zinc-ion storage. *Chin. J. Chem. Eng.* (in press). doi: 10.1016/j.cjche.2020.05.015

Wang, Y., Wang, C., Ni, Z., Gu, Y., Wang, B., Guo, Z., et al. (2020c). Binding zinc ions by carboxyl groups from adjacent molecules toward long-Life aqueous zinc-organic batteries. *Adv. Mater.* 32, 1–8. doi: 10.1002/adma.202000338

Xie, D., Hu, F., Yu, X., Cui, F., Song, G., and Zhu, K. (2020). High-performance Na1.25V3O8 nanosheets for aqueous zinc-ion battery by electrochemical induced de-sodium at high voltage. *Chinese Chem. Lett.* (in press). doi: 10.1016/j.cclet.2020.02.052

Xu, F., Zhai, Y., Zhang, E., Liu, Q., Jiang, G., Xu, X., et al. (2020). Ultrastable surface-dominated pseudocapacitive potassium storage enabled by edge-enriched N-doped porous carbon nanosheets. *Angew. Chem. Int. Ed.* 59, 2–10. doi: 10.1002/anie.202005118

Xu, L., Zhang, Y., Jiang, H., Zheng, J., Dong, X., Hu, T., et al. (2020). Facile hydrothermal synthesis and electrochemical properties of (NH4)2V6O16 nanobelts for aqueous rechargeable zinc ion batteries. *Coll. Surfaces A* 593:124621. doi: 10.1016/j.colsurfa.2020.124621

Yan, M., He, P., Chen, Y., Wang, S., Wei, Q., Zhao, K., et al. (2018). Water-lubricated intercalation in V2O5·nH2O for high-capacity and high-rate aqueous rechargeable zinc batteries. *Adv. Mater.* 30:1703725. doi: 10.1002/adma.201703725

Yang, G., Li, Q., Ma, K., Hong, C., and Wang, C. (2020). The degradation mechanism of vanadium oxide-based aqueous zinc-ion batteries. *J. Mater. Chem. A* 8, 8084–8095. doi: 10.1039/d0ta00615g

Yang, G., Wei, T., and Wang, C. (2018). Self-healing lamellar structure boosts highly stable zinc-storage property of bilayered vanadium oxides. *ACS Appl. Mater. Interfaces.* 10, 35079–35089. doi: 10.1021/acsami.8b10849

Yang, Y., Tang, Y., Fang, G., Shan, L., Guo, J., Zhang, W., et al. (2018). Li+ ions intercalated V2O5nH2O with enlarged layered spacing and fast ions diffusion as aqueous zinc ion battery cathode. *Energy Environ. Sci.* 11, 3157–3162. doi: 10.1039/C8EE01651H

Zampardi, G., and La Mantia, F. (2020). Prussian blue analogues as aqueous Zn-ion batteries electrodes: current challenges and future perspectives. *Curr. Opin. Electrochem.* 21, 84–92. doi: 10.1016/j.coelec.2020.01.014

Zhang, N., Chen, X., Yu, M., Niu, Z., Cheng, F., and Chen, J. (2020). Materials chemistry for rechargeable zinc-ion batteries. *Chem. Soc. Rev.* 49, 4203–4219. doi: 10.1039/c9cs00349e

Zhang, N., Dong, Y., Jia, M., Bian, X., Wang, Y., Qiu, M., et al. (2018). Rechargeable aqueous Zn-V2O5 battery with high energy density and long cycle fife. *ACS Energy Lett.* 3, 1366–1372. doi: 10.1021/acsenergylett.8b00565

Zhang, N., Dong, Y., Wang, Y., Wang, Y., Li, J., Xu, J., et al. (2019a). Ultrafast rechargeable zinc battery based on high-voltage graphite cathode and stable nonaqueous electrolyte. *ACS Appl. Mater. Interfaces* 11, 32978–32986. doi: 10.1021/acsami.9b10399

Zhang, N., Jia, M., Dong, Y., Wang, Y., Xu, J., Liu, Y., et al. (2019b). Hydrated layered vanadium oxide as a highly reversible cathode for rechargeable aqueous zinc batteries. *Adv. Funct. Mater.* 29:1807331. doi: 10.1002/adfm.201807331

Conflict of Interest: The authors declare that the research was conducted in the absence of any commercial or financial relationships that could be construed as a potential conflict of interest.

Copyright © 2020 Qin, Wang, Sun, Lu, Omar and Mikhailova. This is an open-access article distributed under the terms of the Creative Commons Attribution License (CC BY). The use, distribution or reproduction in other forums is permitted, provided the original author(s) and the copyright owner(s) are credited and that the original publication in this journal is cited, in accordance with accepted academic practice. No use, distribution or reproduction is permitted which does not comply with these terms.